



**HAL**  
open science

## Towards a better understanding of grass bed dynamics using remote sensing at high spatial and temporal resolutions

Menu Marion, Papuga Guillaume, Andrieu Frédéric, Debarros Guilhem,  
Fortuny Xavier, Alleaume Samuel, Estelle Pitard

### ► To cite this version:

Menu Marion, Papuga Guillaume, Andrieu Frédéric, Debarros Guilhem, Fortuny Xavier, et al.. Towards a better understanding of grass bed dynamics using remote sensing at high spatial and temporal resolutions. *Estuarine, Coastal and Shelf Science*, 2021, 251, pp.107229. 10.1016/j.ecss.2021.107229 . hal-03125706

**HAL Id: hal-03125706**

**<https://hal.inrae.fr/hal-03125706>**

Submitted on 9 Jun 2021

**HAL** is a multi-disciplinary open access archive for the deposit and dissemination of scientific research documents, whether they are published or not. The documents may come from teaching and research institutions in France or abroad, or from public or private research centers.

L'archive ouverte pluridisciplinaire **HAL**, est destinée au dépôt et à la diffusion de documents scientifiques de niveau recherche, publiés ou non, émanant des établissements d'enseignement et de recherche français ou étrangers, des laboratoires publics ou privés.

1 Title: Towards a better understanding of grass bed dynamics using remote sensing at high  
2 spatial and temporal resolutions

3

4 Authors: Menu Marion<sup>12</sup>, Papuga Guillaume<sup>345</sup>, Andrieu Frédéric<sup>4</sup>, Debarros Guilhem<sup>4</sup>,  
5 Fortuny Xavier<sup>6</sup>, Alleaume Samuel<sup>1</sup>, Pitard Estelle<sup>27</sup>

6

7 1. UMR TETIS, INRAE, AgroParisTech, CIRAD, CNRS, Université de Montpellier, 500 rue  
8 Jean-François Breton, 34093 Montpellier Cedex 5, France

9 2. UMR 5221 Laboratoire Charles Coulomb, CNRS, Université de Montpellier, Batiment 13,  
10 Campus Triolet, Université de Montpellier, CC069, 34095 Montpellier, France

11 3. UMR 5175 Centre d'Écologie Fonctionnelle et Évolutive, CNRS, 1919 route de Mende,  
12 34293 Montpellier cedex 5, France.

13 4. Conservatoire Botanique National Méditerranéen de Porquerolles, antenne Languedoc-  
14 Roussillon, parc scientifique Agropolis-B7, 2214 boulevard de la Lironde, 34980 Montferrier  
15 sur Lez, France

16 5. UMR AMAP, Université de Montpellier, IRD, CNRS, CIRAD, INRAe, Montpellier,  
17 France.

18 6. ADENA, Réserve Naturelle Nationale du Bagnas, Agde, France

19 7. Department of Environmental Science, Policy and Management, University of California,  
20 Berkeley, CA 94720, USA

21

22 Orcid:

23 – Papuga G.: <https://orcid.org/0000-0002-7803-2219>

24 – Alleaume S.: <https://orcid.org/0000-0002-9200-8338>

25 **Abstract**

26 Wetlands conservation and resilience capacities are key issues in many places over the globe.  
27 Understanding these issues will benefit from a precise knowledge of seagrass species  
28 occupancy and coverage over time and over space. Such information can be obtained from  
29 remote sensing images and their classification thanks to a vegetation index, to be used in a  
30 complementary manner to field work inventories. Sentinel-2 data, which are available with a  
31 frequent revisit time (<5 days) and a high spatial resolution (10m pixel size) can be used to  
32 map grassbeds at the surface or slightly below the surface of permanent lagoons, hence  
33 enabling the characterization of its seasonal dynamics, which was not possible with previous  
34 remote-sensing tools. We have proved the feasibility of such a method in the natural reserve  
35 of the Bagnas (Herauld, France) where *Stuckenia pectinata* coverage can be tracked over a  
36 full year thanks to Sentinel-2 images and field work. Inter-annual dynamics (seasonal growth  
37 and senescence) can be mapped over time with 10m resolution and will be extended to  
38 pluriannual studies thanks to the long-term objective of the Sentinel-2 mission. This opens the  
39 way to a concerted management of natural reserves based on data analysis and field  
40 knowledge, a better understanding of seagrass coverage with fluctuating environmental  
41 conditions, and predictive mechanistic and/or stochastic models of future qualitative trends.

42

43

44 Keywords: Remote sensing – temporal survey – mesohaline lagoon – National Natural  
45 Reserve of the Bagnas (France) – pondweed grass beds – Sentinel-2 satellites – *Stuckenia*  
46 *pectinata* – ecosystem management – ecological indicator – wetlands conservation

47

48

## 49 **Introduction**

50 Wetland conservation has become a cornerstone of conservation biology, as these  
51 habitats represent high biodiversity areas, and critical human resources in terms of water  
52 (Pereira et al., 2009), food supply, and eventually recreational areas (Newton et al., 2018).  
53 Consequently, they are under global pressure due to the intensive use of water and change of  
54 soil occupation, which both threaten wildlife and disrupts ecosystem services (Gaertner-  
55 Mazouni and De Wit, 2012). Coastal lagoons are transition waters between continental and  
56 marine domains, filled with brackish water in which salinity may vary over time. They  
57 exemplify wetland conservation issues since they are highly diversified habitats of significant  
58 conservation value (Pérez-Ruzafa et al., 2011). At the same time, they have to face ever-  
59 increasing human impacts due to the development and urbanization of coastal areas (Pojana et  
60 al., 2007) and land use throughout the catchment area (Cañedo-Argüelles et al., 2012; Shili et  
61 al., 2007). Lagoons also represent essential habitats for a variety of taxa: they are a privileged  
62 stopover for migrating birds (Holm and Clausen, 2006); they constitute nurseries for sea  
63 fishes (Yamamuro, 2012); they host many plants (both angiosperms and algae) specific to  
64 these habitats (Hartog, 1981). Variation in salt concentration is a significant determinant of  
65 ecosystem functioning and profoundly impacts biodiversity. Thus, water input shapes the  
66 biodiversity of such ecosystems and can trigger drastic changes over short periods (Obrador  
67 and Pretus, 2010; Shili et al., 2007; Antunes et al., 2012).

68 International awareness of those conservation issues has led to the introduction of  
69 protection treaties, such as the Ramsar treaty (Gardner and Davidson, 2011). At the European  
70 level, two directives have been set up to protect those habitats. First, the Water Framework  
71 Directive (WFD) aims at preserving European waters in a good quality state (Chave, 2001).  
72 This convention covers all water bodies from rivers to lakes larger than 0,5 km<sup>2</sup>, including  
73 coastal lagoons. In parallel, the Habitats Directive (HD) has defined a list of protected habitats  
74 and aims at maintaining their good conservation status to preserve wildlife over long time  
75 periods. Lagoons represent one particular habitat, named "habitat 1150 – Coastal lagoon".  
76 Additionally, different national initiatives have added layers to the protection of such areas. In  
77 France, the National Natural Reserve network includes several lagoons, which ensures land  
78 protection and allows the implementation of management plans tackling biodiversity issues  
79 (Therville et al., 2012).

80 Within lagoons, grass beds represent a key compartment of the ecosystem. They are  
81 primary producers that provide food and produce oxygen, which is essential to many  
82 organisms (Camacho et al., 2012; Scheffer, 1997). They constitute shelters for a whole range  
83 of animals, including fishes and invertebrates (Benedetti-Cecchi et al., 2001; Lloret and  
84 Marín, 2009). The analysis of their composition and dynamics inform on the ecosystem  
85 functioning, regarding both abiotic compartment of the ecosystem (*e.g.* water and soil  
86 characteristics) and biotic interactions (Camacho et al., 2012). Water quality strongly  
87 influences grass beds, as salt and trophic levels influence plant development and survival  
88 (Obrador and Pretus, 2010). Eutrophication is a critical issue as it might lead to a dystrophic  
89 crisis when oxygen decreases to the point where wildlife dies because of anoxic conditions  
90 (Duarte et al., 2002). Such changes in abiotic conditions can lead to sharp temporal transitions  
91 in plant community composition and structure (*i.e.* grassbed extent) that in return deeply  
92 modify the functioning of the whole waterbed (Obrador and Pretus 2010, Antunes et al. 2012,  
93 Perez-Ruzafa et al, 2011), including nutrient cycling (Duarte et al. 2002). Therefore,

94 understanding grass bed dynamics is an efficient surrogate to ecosystem functioning and is a  
95 prime indicator to manage such a system.

96 Legal protection usually assigns biodiversity management as the primary mission of  
97 protected areas, intending to ensure the long-term persistence of biodiversity on the territory.  
98 Implementing efficient conservation strategies requires accurate tools to detect the effect of  
99 changes in the system, and grass beds represent key indicators to understand ecosystem  
100 dynamics. However, quantifying grass beds dynamics is a complex task, due to the inherent  
101 difficulty to access such vegetation (Silva et al. 2008), and assess such highly varying intra-  
102 annual dynamics through the required frequent temporal revisits (Shili et al., 2007; Antunes et  
103 al., 2012). Additionally, the protection status of some lagoons prohibits the use of intrusive  
104 and destructive sampling methods, and restrain access to such areas to limit disturbance of  
105 animals. Collecting and maintaining up-to-date and regular information on grassbed  
106 distribution is a major challenge (Antunes et al. 2012).

107 In this context, the use of remote sensing is a powerful way to characterize the  
108 dynamics of such vegetation without impacting this environment. Lagoons were among the  
109 first to be studied when remote sensing methods emerged 20 years ago (see the review on  
110 pioneering works by Lehmann and Lachavanne, 1997). At that time, those new methods had  
111 to face sharp criticisms because they were expensive (Silva et al., 2008) and produced  
112 inaccurate results (Cazals et al., 2016; Vis et al., 2003). These approaches have seen their  
113 performances rapidly improving over the last ten years and are now increasingly used in  
114 ecological researches (Veetil et al, 2020). Yet, such methods have failed so far to enter the  
115 current monitoring scheme of most natural reserves due to their high cost and complexity of  
116 treatment. Moreover, studies either focused on high resolution/low frequency (*i.e.* once a  
117 year) data (*e.g.* Khanna 2011, which uses a hyperspectral detector able to distinguish between  
118 different species of seagrass), or low resolution/high frequency data, typically based on  
119 Landsat images (Lyons et al, 2013)

120 Today, the emergence of new satellites that produce repeated images free of cost  
121 boosts the development of such technology, and allow ecologists to get insights into seasonal  
122 dynamics of grass beds, a dimension that was hardly accessible before (Traganos et al 2018,  
123 Kohlus et al, 2020). In particular, as part of the European Union Copernicus program, the two  
124 Sentinel-2 satellites produce images every 5 days, at a high spatial resolution of 10 m. Each  
125 satellite carries a single multispectral instrument with 13 spectral channels within visible,  
126 near-infrared, and shortwave infrared spectra, which are particularly adapted to detect  
127 vegetation. This massive flow of earth observation data provides a rich and detailed  
128 description of ecosystems, allowing their condition and evolution to be monitored. It is thus  
129 possible to analyze intra- and inter-annual changes in ecosystems at a fine-scale or monitor  
130 the evolution of the phenology of various ecosystems. The seasonal dynamics of intertidal  
131 grassbeds was investigated in Zoffoli et al, 2020, at low tide.

132 Through this article, we model the growth and persistence dynamics of lagoon grass  
133 beds using remote sensing approaches based on images from the Sentinel-2 satellite, and we  
134 choose the Bagnas Natural Reserve located in the south of France as a model ecosystem. We  
135 model the intra-annual (*i.e.* seasonal) dynamics of such a system during the year 2017 thanks  
136 to high quality repeated images produced every two weeks. Firstly, we differentiate aquatic  
137 vegetation (which can be either submerged or lying at the water surface) from peripheric  
138 reedbeds belts to precisely delimit the open-water lagoon extent. Secondly, we develop two  
139 approaches to delineate grass beds based on simple spectral indices thresholds and Spectral

140 Linear Unmixing approaches. Finally, we compare these two approaches and validate them  
141 with a field map realized in summer 2017 to assess the accuracy of our methods. We discuss  
142 how such a methodology can be extended to other lagoon ecosystems worldwide.

143

## 144 **Materials & methods**

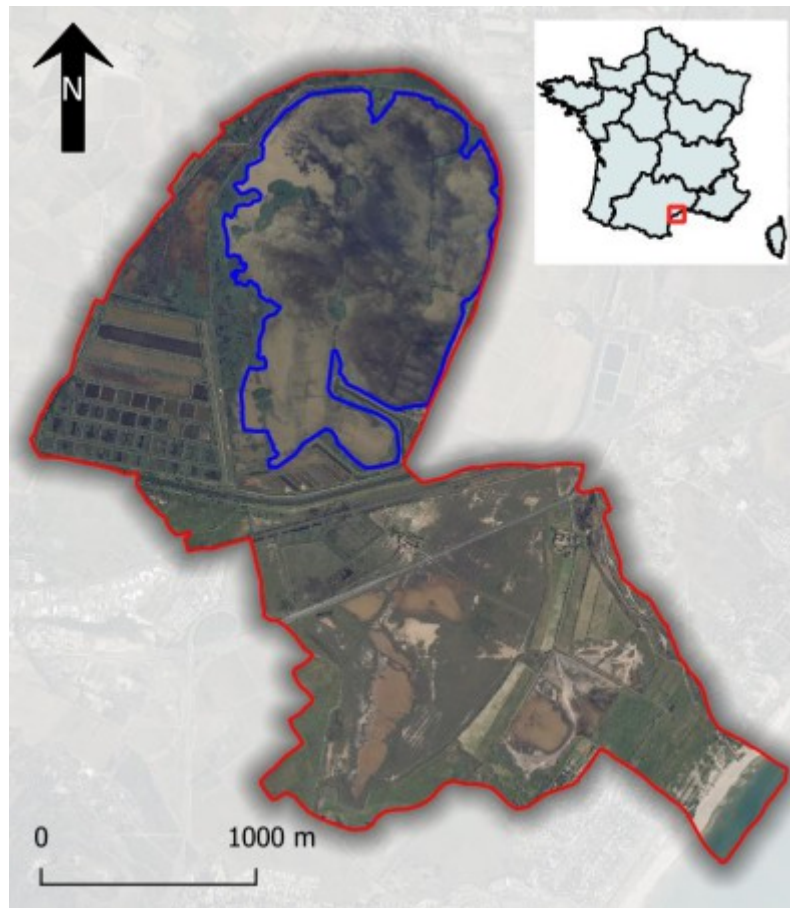
### 145 1. Study site

146 Coastal lagoons are well represented in the south of France, especially west of the  
147 Rhône delta (*i.e.* the Camargue region) where the coast (*i.e.* Gulf of Lion) is formed by  
148 sedimentary deposits. Located in the city of Agde (Hérault, France), the Bagnas (Figure 1) is  
149 a National Natural Reserve since 1983 and Natura 2000 site since 2004. It is composed of  
150 several lagoons of various sizes whose functioning includes temporary and permanent water  
151 bodies. The central lagoon (named "Grand Etang du Bagnas") is a coastal lagoon of  
152 approximately 190 ha. The catchment area measures 805 ha, and is mostly occupied by  
153 agricultural activities (including vineyard) and urbanization.

154 Most of the water supply (66%) corresponds to freshwater coming from the Hérault  
155 stream through the Canal du Midi (Agbanrin, 2018). The rest is brought by rainwater (34%).  
156 The lagoon is hydraulically managed to preserve qualitatively biodiversity issues, especially  
157 for water birds. This management consists mainly of controlling inflows and outflows to  
158 maintain water levels compatible with the ecological requirements of species. As a result,  
159 water levels are maintained at about 85 cm between December and March to support  
160 wintering stationing of waterbirds species. From the beginning of spring, the water levels are  
161 lowered until reaching 40 cm in August to allow the nesting of specific target species and also  
162 to make the lagoon attractive for migratory birds next fall (however, there are fluctuations and  
163 discrepancies between target water levels and measured water levels, see Appendix 1). Thus,  
164 its salinity is comprised between 5 and 20g/L, and fluctuates throughout the year depending  
165 on water inputs, making it a mesohaline lagoon (Grillas et al., 2018).

166 The lagoon is surrounded by reed beds and is extensively covered by a grass bed  
167 almost exclusively composed of pondweed (*Stuckenia pectinata* (L.) Börner 1912). The grass  
168 bed stretches to its maximum extent during the summer (August-September) and disappears  
169 during winter. When plants reach their maximum development, their leaves attain the surface  
170 and entirely cover parts of the water body. It constitutes an essential resource for migratory  
171 birds, especially ducks that feed on leaves and/or seeds (Arzel et al., 2006). Two other species  
172 can be occasionally found: *Ruppia cirrhosa* (Petagna) Grande, 1918 is an angiosperm sparsely  
173 distributed throughout the lagoon, most of the time represented by few individuals;  
174 *Lamprothamnium papulosum* (K.Wallroth) J.Groves, 1916 is a *Characeae* that occasionally  
175 appears below grass beds, and never reaches the surface.

176



178  
 179 Figure 1: Map of the Bagnas Reserve region of interest. The full reserve limit is in  
 180 red, while the Grand Bagnas where our study focuses is limited by the blue line.

181  
 182 2.Satellite images

183 To detect grass beds, we used Sentinel-2 multispectral images with 10m resolution  
 184 bands: blue (B2), green (B3), red(B4), and near-infrared NIR (B8). These images are  
 185 produced by two satellites (Sentinel 2A and 2B) launched by the European Spatial Agency  
 186 (ESA) thanks to the Copernicus program of the European Union. They allow accessing  
 187 images of the same area every 5 days. ESA produces and distributes Level 1C ortho-rectified  
 188 data expressed in reflectance at the top of the atmosphere. Theia platform (theia.cnes.fr)  
 189 produces and distributes level 2A data, corrected for atmospheric effects thanks to the MAJA  
 190 software (Hagolle et al., 2017). This processor uses multi-temporal information to detect  
 191 clouds and clouds' shadows to estimate the optical properties of the atmosphere. Thanks to the  
 192 high temporal frequency of the Sentinel-2 instrument, we could work with a temporal series  
 193 of 32 high-quality cloud-free images taken between January 13<sup>th</sup> 2017, and April 13<sup>th</sup> 2018.  
 194 Early 2018 images were conserved to assess the date of minimal expansion of the grassbed, as  
 195 mediterranean winter does not coincide strictly with calendar year.

196  
 197 3.Field data

198 During summer 2017, we launched a field campaign to map the distribution of the  
 199 grass bed. We set up 103 sampling points following a systematic grid of 200m, doubled

200 within the first 100m from the pond border to improve the detection of vegetation variability  
201 (personal communication P. Grillas, 2016). Each point was sampled by boat at the end of July  
202 2017; first, we recorded the frequency of each species of the community based on 5 samples  
203 collected with a rake all around the boat. Second, we evaluated the grass bed cover by giving  
204 6 estimations of its total cover within 6 sectors around the boat (Appendix 2). All estimation  
205 was made by the same person, based on a simple scale to classify the grass bed as absent (no  
206 plants), rare (0-25%), abundant (25-50 %), or very abundant (>50%). The median of those  
207 classes was averaged to obtain one cover estimate per sampling station (following van der  
208 Maarel 1979). At the same time, we measured the depth at each sampling point with a rigid  
209 meter (precision ~ 1cm) and used linear interpolation to create a bathymetric map.

210

#### 211 4. Remote sensing mapping of grass bed

##### 212 4a. Preliminary treatment

213 Thirty-two Sentinel-2 images were downloaded from the Theia platform and clipped  
214 with the *gdalwarp* tool from the library *gdal* (GDAL/OGR contributors, 2020) according to  
215 the region of interest. The four 10 m bands (B2, B3, B4, B8) of each image were then  
216 concatenated to i) create a series of color composite and ii) to calculate spectral indices over  
217 the lagoon area. The color composite consists of a combination of bands to better visualize  
218 and photo-interpret the satellite image. Two-color composites were derived. The first one, a  
219 true-color imagery, was displayed in a combination of red, green, and blue band, and the  
220 resulting image was reasonably close to reality. The second, a false-color image, was built  
221 with band 2 displayed in blue, band 3 in green, and band 4 in red. Vegetation appears in bright  
222 red as green vegetation readily reflects infrared light energy.

223 Then, we computed several different radiometric indexes to select the one that allowed  
224 to better-distinguished water from vegetation (see Appendix 3 for details). We retained the  
225 Modified Soil Adjusted Vegetation Index 2 (MSAVI2) (Qi et al., 1994) according to our  
226 observations and in agreement with the literature (Calleja et al., 2019; Colditz et al., 2018;  
227 Bradley et al., 2004). It was calculated with the formula:

$$228 \quad MSAVI2 = \frac{2 * NIR + 1 - \sqrt{(2 * NIR + 1)^2 - 8 * (NIR - R)}}{2}$$

229 where NIR and R are respectively the near-infrared and red band reflectances.

230 Additionally, we generated a map of the MSAVI2 variance to distinguish vegetation types  
231 based on their variability over the studied period and studied area.

232

##### 233 4b. Pixel interpretation and sampling method

234 Our approach is based on the interpretation of pixels based on true and false-color  
235 images composites, MSAVI2 index, and variance of the MSAVI2 throughout the year.  
236 Though the definition of classes can be difficult, we propose a simple scheme that describes 3  
237 classes to classify pixels that belong to three compartments of the lagoon, namely reedbeds  
238 (R), grassbeds (G), and water (W). Reedbeds form a belt around the lagoon; they appear  
239 clearly in true color maps and present the lowest variability over the time, as they are  
240 helophytes that maintain a minimal photo-activity all year long.

241 Based on our field study and local knowledge from reserve managers, we assumed that  
242 grass beds are dominated by one single aquatic species (*Stuckenia pectinata*). According to  
243 the season, pond grass can be either absent, submerged (early stages of growth), or emerged



244 on the surface of the lagoon (later stages of growth). Thus we identified pondweed grass bed  
245 pixels as being variable through the year and exhibiting high MSAVI2 values during summer.  
246 True color images taken during summertime allowed us to identify large continuous patches  
247 of grass bed in which we selected our pixels.

248 Finally, we characterized water pixels as being the least variable, with low MSAVI2  
249 values and being blue in true color. They remain water pixels on the whole series of images.  
250 We sampled a number of photointerpreted polygons from each category. Appendix 4 shows  
251 the photo-interpreted pixels.

252

#### 253 4c. Temporal profile of MSAVI2 and threshold classification method

254 The objective was to delimit ecosystem compartments. To do so, we extracted the  
255 MSAVI2 value of all reference pixels throughout the temporal series of images and plotted it  
256 to create compartment profiles for R, W, and G. Then, we visually investigated the curves to  
257 consider whether or not we could separate the signatures from each class.

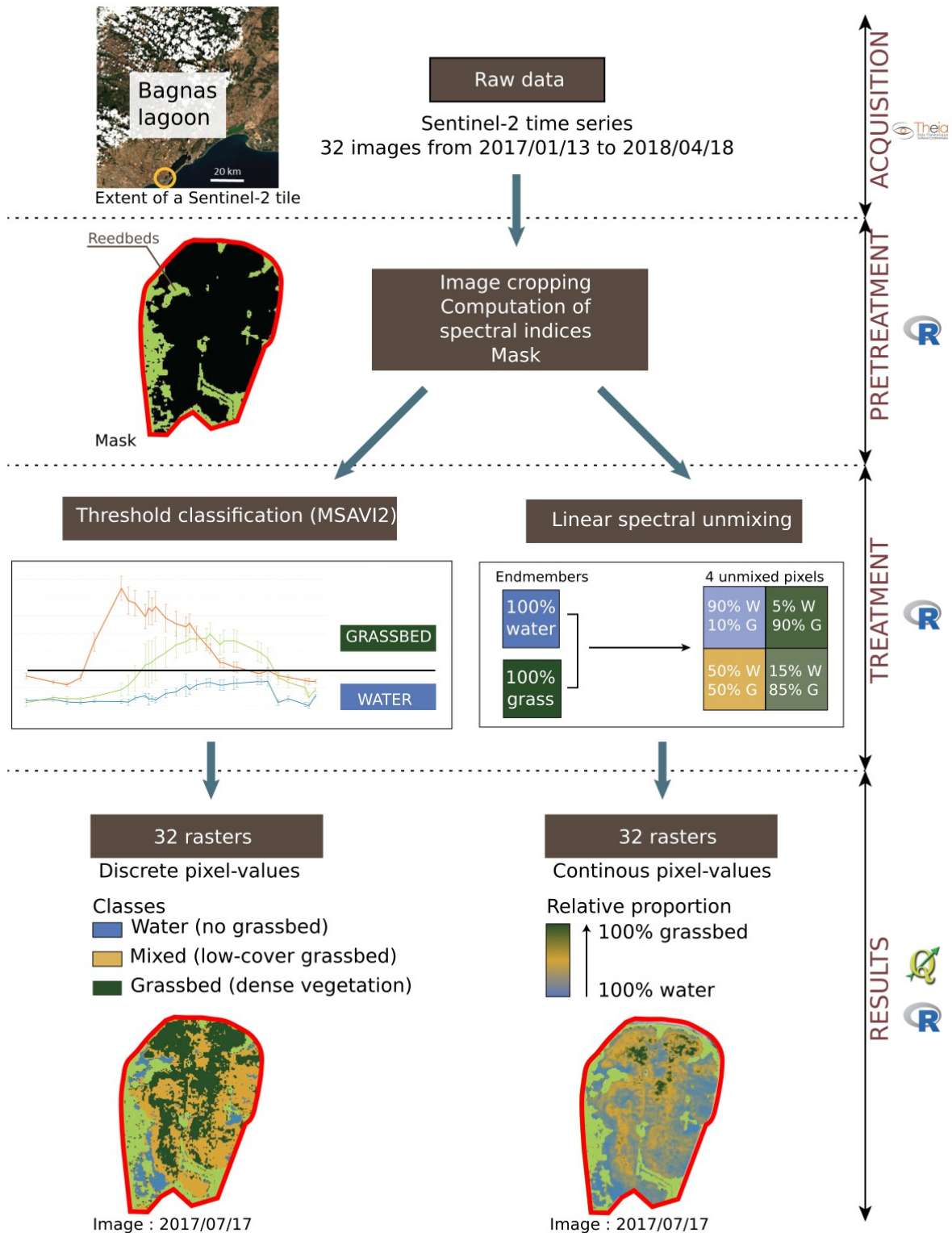
258 First, we had to delimit the open water part of the lagoon and exclude surrounding  
259 reedbed belt to create a water body mask, as pixels identified as reedbed would be used as a  
260 mask to explore only G inside the water body. Reedbeds are vegetation whose occupancy  
261 remains globally stable during one vegetative season. Thus, we chose one image that presents  
262 the biggest difference between reedbed MSAVI2 values and all other compartments of the  
263 ecosystem, to fix a threshold we later applied to the whole series of images across the lagoon.  
264 In the second part, we aimed at mapping the occupancy of grass bed by discriminating W  
265 from G. G fluctuate along the year, as aquatic vegetation grows during the spring and decline  
266 in winter, stopping all photosynthesis. Yet, W pixels were chosen because they stayed stable  
267 and presented nearly no photosynthetic activities during the year. Therefore, we fixed the  
268 lower threshold below which a pixel is considered as water as the highest value of the mean  
269 W series (see Cazals et al., 2016). Preliminary results showed us that the maximum  
270 development of the grass bed was around August-September, so we similarly fixed the  
271 threshold above which a pixel is considered G as the lowest mean value of the series.

272 While W and G classes could be clearly identified using photo interpretation, the  
273 values between the two thresholds corresponded to different types of aquatic vegetation:  
274 sparse grass bed, growing grass bed, or mixed-pixels that contained both developed grass bed  
275 and water in various proportion. We have chosen not to assign those pixels to one or the other  
276 category, so we assigned a mixed (M) class is to every pixel in which index value lies in  
277 between these 2 thresholds.

278

#### 279 4d. Spectral Linear Unmixing (SLU) classification method

280 The Spectral Linear Unmixing (SLU) method provides a continuous description of  
281 each pixel in terms of a percentage of 2 pure endmembers and is commonly used in (Keshava  
282 and Mustard, 2002; Wikantika et al., 2002). We used the R *hmisc* library for spectral linear  
283 unmixing between 2 endmembers (Harrell Jr, 2018). The chosen endmembers were  
284 respectively W and G, which spectral signatures were sampled using the 4 bands on photo-  
285 interpreted pixels chosen in 17 different images of the time series (42 pixels for W, and 52  
286 pixels for G). After the unmixing analysis, each pixel in each image is assigned a percentage  
287 of W content and G content, resulting in a continuous gradient of aquatic vegetation content  
288 between the 2 pure endmembers. The analysis workflow was written and run using the free  
289 software R and QGIS. Figure 2 illustrates the general implementation scheme of the method.



291  
292 Figure 2: General data workflow scheme.

293  
294  
295

296

## 297 5. Statistical analysis

### 298 5a. Conformity of the two modeling approaches

299 We compared the conformity of the two approaches by plotting for each pixel the  
300 value extracted from the SLU method against the corresponding category (W-M-G) defined  
301 through the threshold approach .

302

### 303 5b. Comparison of field data and modeled grass bed maps

304 To compare the accuracy of field and modeling approaches, we modeled the fit of our  
305 results based on remote-sensing with field maps established during summer 2017. To account  
306 for localization mismatch, we extracted for each sampling point the modeling output of each  
307 of the nine 10\*10m pixels centered around the GPS points, for both threshold and unmixing  
308 approaches. Field sampling took place on July 29<sup>th</sup> 2017, so we extracted corresponding  
309 values from the closest image captured on August 08<sup>th</sup> 2017.

310 For the threshold method, values extracted from pixels were categorical. For each field  
311 sampling point, we calculated the proportion of each category (W, M, G) out of the 9  
312 corresponding pixels. Then we fitted a generalized linear model for each category, with the  
313 proportion of pixels as the response variable and the field estimate as the explanatory variable.  
314 We used a quasi-binomial probability density function as preliminary analysis showed high  
315 overdispersion in the data.

316 For W, we expected a decrease of W-pixels proportion with denser vegetation cover;  
317 for G, we expected the reverse trend. Then, the proportion of mixed-class pixels was supposed  
318 to peak for intermediate field values, representing sparse grass beds. Thus, we added to the  
319 model a polynomial term with the square of the field value as an explanatory variable.

320 For the SLU method, values extracted from pixels were continuous. We averaged the  
321 nine values and ran a generalized linear model with the field-estimated cover of the grass bed  
322 as the response variable, and the averaged modeled value as the explanatory variable. We also  
323 used a quasi-binomial probability density functions for similar reasons.

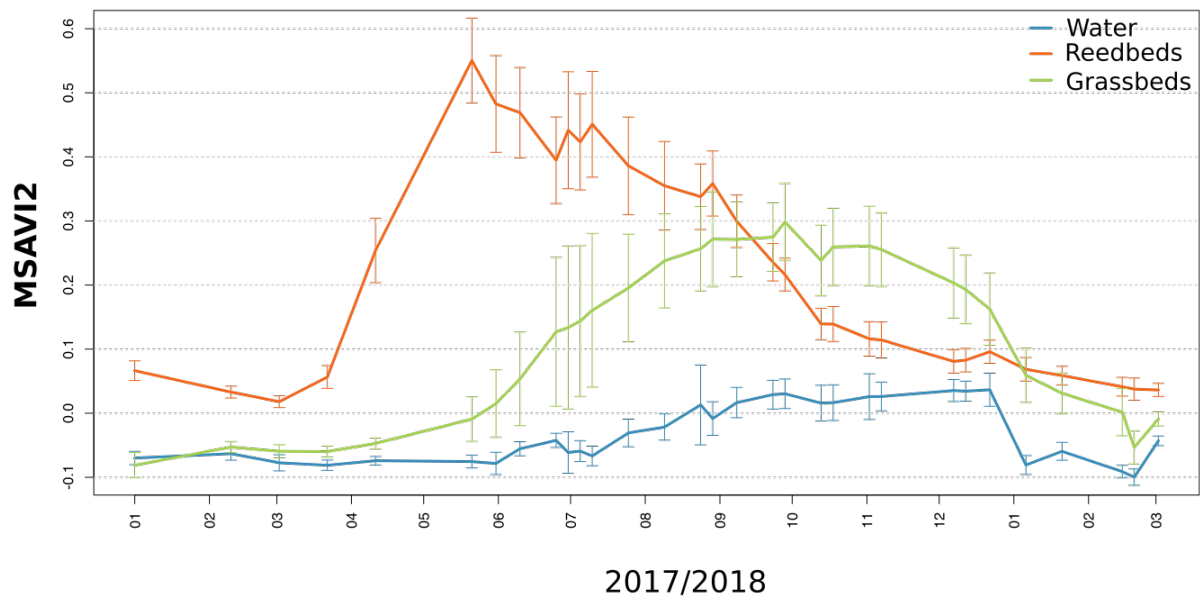
324 For each model, the significance of each explanatory variable was investigated thanks  
325 to a t-test implemented in the "summary" function in R (R Core Team 2019).

326

## 327 **Results**

### 328 1. Time variation of the MSAVI2 index

329 The MSAVI2 profile for water is distinct from the profiles of aquatic vegetation  
330 (Figure 3). Reed, however, can have an index value comparable to aquatic vegetation and has  
331 to be considered separately. Aquatic vegetation has an annual index profile showing a  
332 minimum in winter, a growth phase, and a maximum saturation state during the summer and  
333 fall. Because patches of aquatic vegetation do not grow synchronously over space, some  
334 aquatic vegetation grows early and emerges in the summer, while others stay submerged  
335 during more prolonged periods. Thanks to this index profile over time, we built a  
336 classification scheme that allows consistently classifying the complete image time-series,  
337 based on the distinction between water, submerged aquatic vegetation, and emerged aquatic  
338 vegetation. The reed beds spatial extent was characterized using (MSAVI2 variance) and the  
339 threshold value of its MSAVI2 index ( $> 0.15$ ) on the June 2<sup>nd</sup> 2017 image as it shows to be  
340 distinct from aquatic vegetation at this date. We used the spatial extent of the reed as a mask  
341 on all the images so that the subsequent analysis was only done on W, M, and G.



343 Figure 3: MSAVI2 Index temporal profile from January 2017 to March 2018.

344

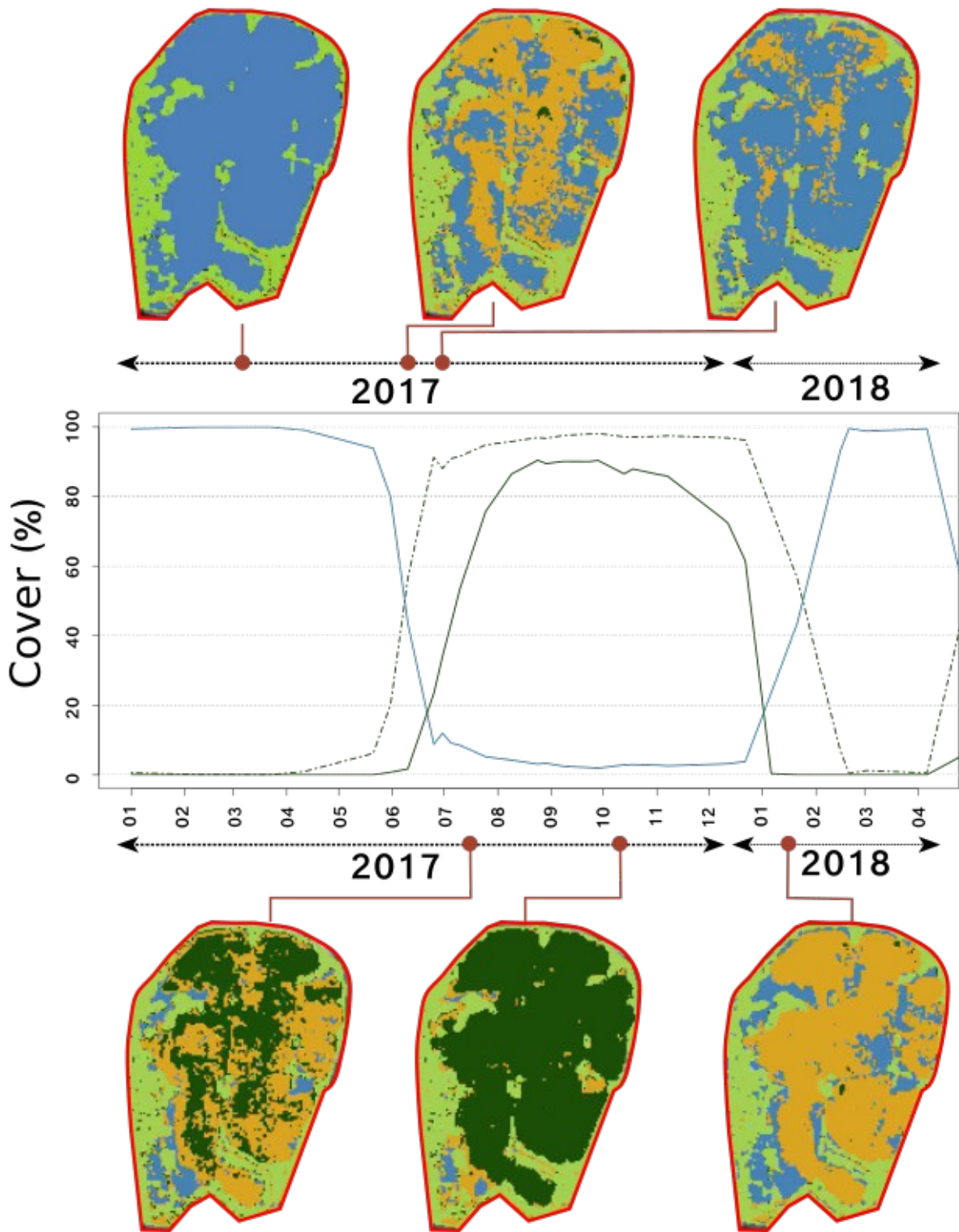
345

346 2. Results from the Threshold Method

347 We used the MSAVI2 profiles to define thresholds to distinguish between the W, M,  
 348 and G classes discretely. While W and G classes can be identified using photointerpretation  
 349 (their MSAVI2 thresholds values being respectively less than 0.025 for W and more than 0.15  
 350 for G), the M class is assigned to every pixel whose MSAVI2 value lies in between these 2  
 351 thresholds. From our field knowledge, we can infer that most of these pixels refer to actual  
 352 submerged aquatic vegetation, with occasional pixels of a mixed boundary phase between  
 353 aquatic vegetation and water, or even pixels of very turbid, nutrient-rich water.

354 The threshold method is efficient in classifying in a discrete way (W, M, G) the  
 355 aquatic vegetation over time. We choose to represent the results at 6 distinct dates  
 356 representative of the seasonal variations of aquatic vegetation development (Figure 4). The  
 357 results of the method are consistent in the sense that each pixel changes class over time in the  
 358 way it should do following the vegetation annual cycle : from W to M (first stage of growth in  
 359 the water) to G (maximum growth), then to M again (start of senescence phase) to W finally.  
 360 The classified maps allow computing the relative areas of the different classes on a single  
 361 graph. Adding the M and G class areas allows computing the global growth starting early  
 362 spring 2017 and leading to the maximal extent at the end of August 2017, which is persistent  
 363 over the whole lagoon until early January 2018. Senescence then starts and continues until the  
 364 end of February 2018, where the lagoon is void of vegetation again. The mixed-phase  
 365 corresponds indeed to submerged aquatic vegetation, and its dynamics allows detecting the  
 366 very early stage of growth of aquatic vegetation. M area shows a peak in early July,  
 367 corresponding to aquatic grass reaching the surface after the subaquatic development phase.  
 368 Since floating aquatic vegetation reflects a radiometric signal different from submerged  
 369 aquatic vegetation, it is then classified as G. At this transition time, the M area starts to grow,  
 370 whereas the G area starts to decrease.

371



373 Figure 4: Classified maps obtained from the threshold method: W (blue), M (orange),  
 374 G (dark green), reedbeds (light green). The blue line represents the water coverage  
 375 over time, whereas the dark green line is the G coverage and the dashed dark green  
 376 line is the (G+M) coverage.

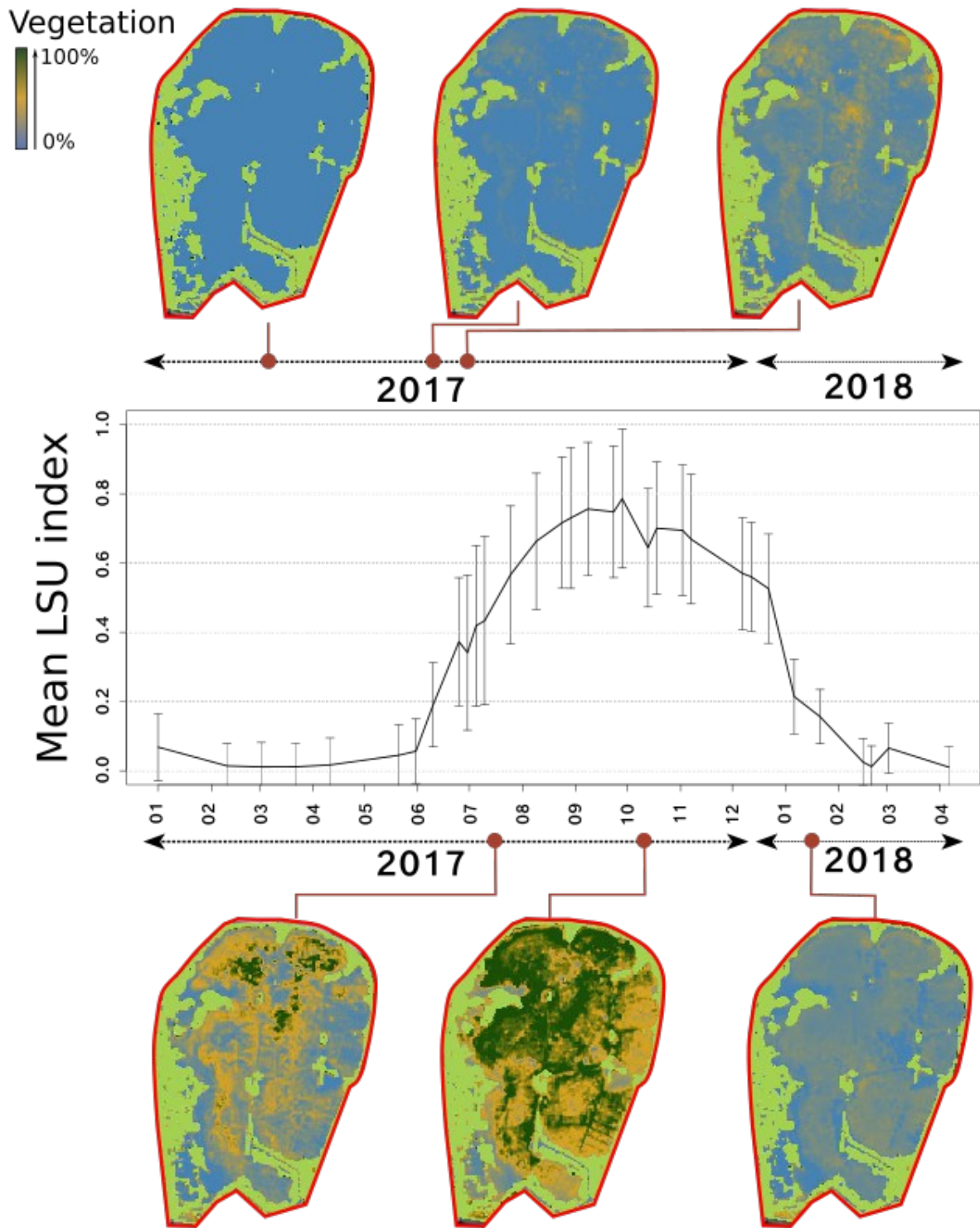
377  
 378

379 3. Results using the Spectral Linear Unmixing (SLU) method

380 This method provides a continuous measure of the aquatic vegetation development  
381 over time, which is presumably proportional to an abundance measure. The dynamics of each  
382 pixel of the studied area is also consistent with the annual vegetation cycle. Figure 5  
383 illustrates how pixels are analyzed using the SLU method and provide maps of a measure of  
384 vegetation abundance over time. The mean LSU index over variable pixels sums up the  
385 seasonal growth and senescence of the grassbeds. Photo-interpreted pixels of W, early G, and  
386 late G (see Appendix 4) are distinct from each other regarding aquatic vegetation content  
387 during the growth phase, and their maximum vegetation content during the summer and fall  
388 are also significantly different (not shown). However, they follow the same mortality curve  
389 during the senescence phase starting in December 2017. Water pixels are somehow analyzed  
390 in an unexpected way, with 40% of aquatic vegetation at the end of the fall, which may  
391 correspond (as it is most likely an artefact of the LSU method) to nutrient-rich content – either  
392 algal bloom or dying aquatic vegetation-(not shown).

393

394



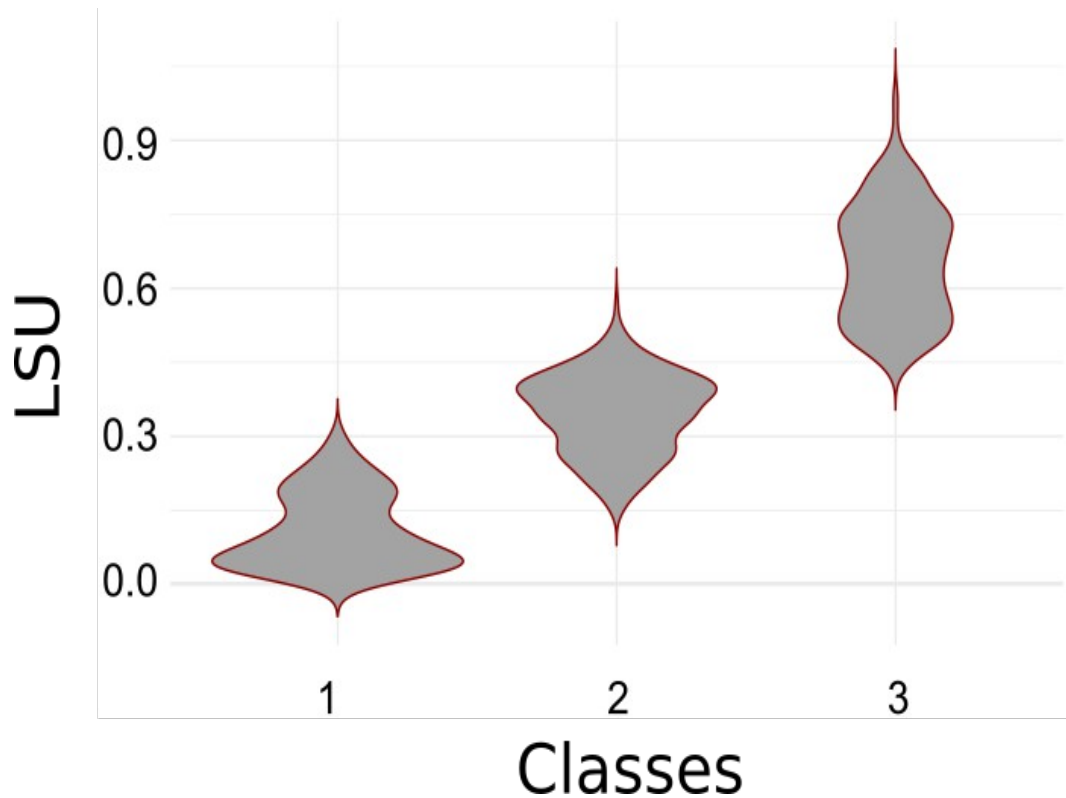
396 Figure 5: Classified maps obtained from the LSU method: W (blue), M (orange), G  
 397 (dark green), reedbeds (light green). The black curve is the mean LSU index  
 398 temporal profile.

399

#### 400 4. Comparison of the two methods

401 The two approaches are globally coherent, as we observed the expected trend of higher  
 402 SLU values in the grass bed category compared to mixed and water. We observed a clear shift  
 14

403 between grass bed (G) and mixed (M) compartment for a SLU value of approximately 0.45.  
404 However, this limit is not perfectly clear between mixed (M) and water (W), as an overlap  
405 appeared for SLU values of 0.15 to 0.3. (Figure 6).  
406  
407



409 Figure 6: Comparison of the concordance of two modelling approaches (Linear  
410 Spectral Unmixing and Classification) to classify Sentinel 2 images into ecosystem  
411 compartments in a coastal lagoon. Violin plots represent the distribution of pixels  
412 value based on the LSU model (y-axis) classified in their related category (x-axis).  
413 Categories represent the three ecosystem compartments: 1 is for water, 2 is for  
414 mixed vegetation, and 3 is for grass bed.

415  
416

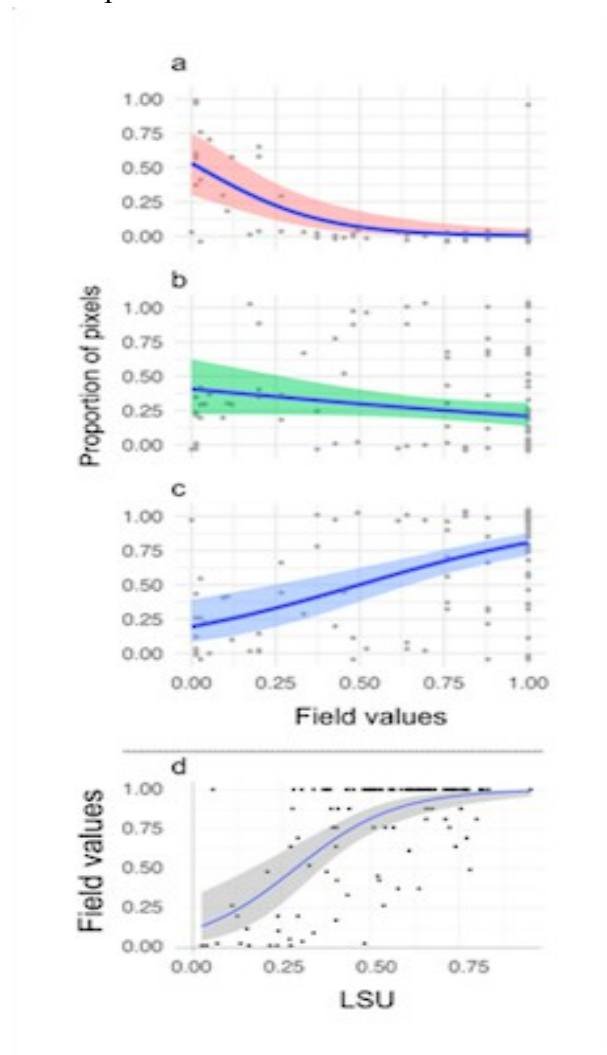
### 417 5. Comparison with field data

418 To analyze the relationship between the proportion of categorized pixels through our  
419 remote sensing approach and the field estimate of grass bed abundance, we ran one test per  
420 category (Figure 7). For W, the proportion of pixels decreased significantly with the increase  
421 of grass bed abundance (coefficient estimate  $\sim -5.5 (\pm 1.98)$ , t-value  $\sim -2.781$ , p-value  $\sim 0.006$ )  
422 as expected. For G, the proportion of pixels increased significantly with the increase of grass  
423 bed abundance (coefficient estimate  $\sim 2.84 (\pm 0.47)$ , t-value  $\sim 6.041$ , p-value  $\sim 1.7e-08$ ) as  
424 expected. For M, we detected a weak decrease in the proportion of pixels against grass bed  
425 abundance (coefficient estimate  $\sim -0.96 (\pm 0.42)$ , t-value  $\sim -2.284$ , p-value  $\sim 0.02$ ) but no peak  
426 as previously expected. Such results have to be considered with care because both models  
427 performed poorly, as reflected in high overdispersion rate found for each one (residual  
428 deviance of 225, 684 and 695 for 112 degrees of freedom, for W, M, and G, respectively),



429 despite the use of quasi-binomial probability density functions. This failure is explained by  
430 the very high skewness toward high values of field data, as presented in Appendix 5.

431 We faced similar issues when running the comparison with LSU. We detected a  
432 significant positive relationship between field estimates of grass bed abundance and LSU  
433 (coefficient estimate  $\sim 7.02 (\pm 1.04)$ , t-value  $\sim 6.77$ , p-value  $\sim 5.02e-10$ ). However, the model  
434 performed poorly as the residual deviance was 5405 on 121 degrees of freedom, which  
435 reflects very important overdispersion in data.



437  
438  
439  
440

441 Figure 7: Comparison plot of field values with results from two modelling approaches  
442 (Linear Spectral Unmixing and Classification). Field samples were geolocated, and  
443 the nine 10\*10m pixels were attributed to the sampling station in order to account for  
444 GPS precision. The top three plots represent the proportion of pixels attributed to  
445 each class (plot a: water, b: mixed vegetation, c: grass bed) as a function of the cover  
446 of grass bed estimated through a field approach. The bottom plot (d) represent the  
447 proportion of grass

448  
449

## 450 **Discussion**

451         Creating reliable ecological indicators is a prerequisite to assess the efficiency of  
452 ecosystem management. Lagoons are dynamic ecosystems of high conservation value, and  
453 monitoring grass bed is paramount to understanding their ecological status. Here we present  
454 an easy-to-handle method that allows managers to survey grass bed development every week  
455 based on the open, free and public satellites image archive of Sentinel-2. This tool allows  
456 reserve managers to survey vegetation at a high spatio-temporal resolution without any  
457 intrusion in the habitat (a crucial aspect in reserves), which limits disturbances of the  
458 ecosystem. The annual dynamics derived by this method and is a prerequisite knowledge to  
459 understand the grassbeds ecosystems over many years, given that it continues to be derived  
460 each year.

461

### 462 **Spatial and temporal dynamic of pondweed grass beds of the Bagnas lagoon**

463         Analyzing the spatial and temporal dynamics of vegetation every week has shed light  
464 on ecosystem dynamics that were hardly approached before (Antunes et al., 2012). In our  
465 case, satellite images were spread during one vegetative year; we detected a late growth by  
466 May and June. This could be due to the management drought generated the previous year (*i.e.*,  
467 *assec* in French) to mineralize the substrate and limit eutrophication. Such perturbation could  
468 have delayed the growth of pondweed and might have extirpated a fraction of the population.  
469 However, previous experiences had shown that most rhizomes remained alive, and individuals  
470 resprouted when water filled up the lagoon (but see also Casagrande and Boudouresque,  
471 2007). This growth was followed by a maximum coverage reached in early August when the  
472 grass bed covered nearly the whole of the water body. Due to summer evaporation and high  
473 density of plants, leaves outcropped at the surface. The grass bed remained in a similar  
474 development state until winter when it slightly decreased. Finally, we did not detect any living  
475 vegetation during the two coldest months of 2018 winter (January-February). However, not  
476 detecting the vegetation is not equivalent to the death of individuals; it's probable that  
477 rhizomes have persisted in the substrate, while leaves died out and decomposed (Casagrande  
478 and Boudouresque, 2007; Van Wijk, 1988).

479         The extent of the grass bed cover is to be compared with past information, although no  
480 formal survey has produced analyzable data. In the early 1990s, the lagoon already contained  
481 a pondweed grass bed, but it was fragmented and patchy. After 10 years, the grass bed  
482 covered most of the water body during summer, and despite some inter-annual variability, it  
483 remained like this until now. *S. pectinata* is a halotolerant species whose growth increases  
484 under eutrophic conditions. Thus, its dominance reveals a high trophic state of the lagoon  
485 (Casagrande and Boudouresque, 2007; Menéndez López and Comín, 1989; Shili et al., 2007),  
486 which could have accumulated nutrients (*i.e. nutrient sink*, Rodrigo et al., 2013) due to small  
487 water inputs and a “saline effect” (*i.e. nutrient accumulation after summer evaporation*),  
488 though some purges are done in the winter and spring in the context of water level  
489 management (Agbarin et al., 2018). The management drought organized every 5 to 10 years  
490 aims at limiting eutrophication by mineralizing the substrate, but it is difficult to assess its  
491 efficiency because of a lack of precise surveys. Furthermore, a reflection is currently  
492 underway by the natural reserve scientific board to move towards a more passive management  
493 of the Bagnas lagoon, which should lead to an increase in water salinity (Agbanrin, 2018).

494 This change in ecological conditions may affect grass bed composition and spatial extent.  
495 Such changes will have to be monitored; therefore, the use of satellite images will constitute a  
496 fundamental tool to understand grass bed response to lagoon management and its overall  
497 impact on vegetation ecosystems.

498

### 499 **A step toward a long-term automated survey of vegetations for conservation**

500 The setting of long-term surveys within protected and managed natural areas is an  
501 essential step toward efficient conservation of ecosystems over time. Such surveys need to  
502 match *several* criteria, among which reproducibility (independence of observer), producing  
503 analyzable data (good statistical power), and low cost are crucial (David, 2005). Such  
504 constraints are even more stringent when quantifying dynamic processes require frequent  
505 resampling over the year. Thus, our approach is free of observer bias and produces two  
506 complementary perspectives of lagoon grass beds over time. These two classification methods  
507 are complementary, and both have their strengths and limits. The threshold method produces  
508 very stable results through time; however, thresholds are applied subjectively, and their  
509 strength *should* be assessed. On the other hand, the SLU method produced results that can be  
510 temporally a bit less coherent: subtle variation in plant growth, or changes in water level, can  
511 affect the reflectance of pixels and modify the calculated vegetation index. The value of  
512 endmembers used to calibrate the algorithm can in principle influence the estimate per pixel.  
513 The 42 pixels of water and 52 pixels of vegetation sampled as end members were selected in a  
514 homogeneous way across the lagoon (hence for different depths and different distances from  
515 the reedbeds borders) and spanning 17 satellite images over time. By analyzing reflectance  
516 values of the pixels for the 4 main bands (RGB and NIR) we noted that their distribution  
517 across pixels could be considered as narrow gaussians. For example, the mean NIR band  
518 reflectance for vegetation endmembers has 0.2176 mean value and 0.0419 standard deviation.  
519 This is somehow consistent with what is expected for « pure » endmembers. However, this  
520 has to be kept in mind and might not be always the case for further uses of « pure »  
521 endmembers across the years or for other lagoons More complex algorithms (such as *Spectral*  
522 *nonlinear unmixing*) might also provide better results. However, the complementarity of the  
523 two methods allows users to select the most adapted metric to their context. Additionally, it is  
524 worth mentioning that this methods could be tested using other spectral information, such as  
525 the red-edge region, where the vegetation reflectance generally increases (Shuster et al.,  
526 2012). The use of the red-edge NDVI index could lead to more refined classification  
527 depending on the context, as shown by Khanna et al. (2011) to distinguish macrophytes in  
528 turbid water; however this study based on plane-embarked hyperspectral tools cannot be  
529 reproduced with a frequency comparable to Sentinel-2 data. Note also that in the study of  
530 intertidal grassbeds of (Zoffoli et al, 2020), the NDVI index was proved to be sufficient for  
531 classification, which is probably due to the very low amount of water present at low tide and  
532 to the fact that no other vegetation seemed to be present. It could be interesting to test the  
533 validity of the MSAVI2 index that we used here in the context of intertidal grassbeds.

534 The integration of remote sensing-based surveys into conservation practices strongly  
535 relies on the use of simple methods, as overwhelming statistical complexity is one of the main  
536 breaks of knowledge transfer from research to applied conservation (Sutherland et al., 2019,  
537 2009). Both methods presented here rely on very simple photointerpretation and basic  
538 knowledge of the lagoon to produce reliable results. The weak correlation observed with field  
539 data points out the weakness of field campaigns to survey such vegetative ecosystems; in

540 particular, the inaccuracy of field estimates to precisely quantify abundance within patches of  
541 high plant density. Non-intrusive estimates realized by sighting alone had a marked tendency  
542 to group all patches of high plant density, which led to an extreme skewness in our field data,  
543 and ultimately did not allow us to fit a representative model. Such skewness also prevented us  
544 from using supervised classification methods. Additionally, localization (due to the boat  
545 moving or drifting while sampling, for example) could have implied critical bias when further  
546 mapping results.

547 Yet, it is essential to mention that remote sensing-based maps represent the  
548 interpretation of a vegetation index based on the chlorophyllous activity of plants, which is  
549 not directly related to the abundance or the density of the plant. For example, pixels classified  
550 as mixed by the threshold method can represent sparse grass bed, dense grass bed but small  
551 plants with more water to the surface, or transition areas between grass bed and bare soil.  
552 Additionally, there is no consensus to link such vegetation index to a particular feature of  
553 vegetation, be it stem density or biomass (Vis et al., 2003).

554

### 555 **Transferability assessment of the method**

556 The Bagnas lagoon has constituted an appropriate training site to develop the method,  
557 as it allowed a precise detection of the grass bed through satellite images. However, the use of  
558 this method in different ecological contexts might require precautions before interpreting  
559 grass bed dynamics. First, the pondweed grass bed of the Bagnas lagoon was highly abundant  
560 and well developed, which allowed satellites to detect a clear photosynthetic signal. Sparse  
561 aquatic vegetation might be more complex to model (Ahmed et al., 2009). Then, the grass bed  
562 was dominated by one single species, which discarded any bias regarding different reflectance  
563 associated with different species. Regarding the structure of the water body, the lagoon is  
564 homogeneously shallow (about 50cm in summer), which limits the impact of water to weaken  
565 the signal. Water was relatively clear, probably as a result of shallow water, high plant density  
566 that limits current and water column that contained little to no suspended sediment (Grillas et  
567 al., 2018; Shili et al., 2007). Finally, no micro-algae bloom occurred during the study period,  
568 an event that can blur the detection of grass bed by increasing the chlorophytic signal.  
569 Therefore, it is likely that the transferability of our approach might require some technical  
570 adaptations to be efficient in different contexts; for example, temporal series of images could  
571 be used to model a pixel-based vegetation index trajectory that could smooth measurement  
572 artifacts.

573

### 574 **Perspectives to understand intra-annual and inter-annual plant growth or persistence**

575 The rise of new ecological data opens new paths to model dynamics at a fine scale.  
576 Maps produced by the SLU method can be used to infer growth parameters (not measurable  
577 by field surveys) that are likely to be heterogeneous in space and likely to depend on the  
578 topographic and environmental parameters of the study site. Population dynamics simulations  
579 can be implemented using these parameters for prediction and management purposes in  
580 different environmental scenarios. This will provide temporal scenarios of plant coverage  
581 based on real data, to be compared to known theoretical cases where the effect of  
582 heterogeneity of growth rates (Hiebler 2004) and connectivity heterogeneity (Gillaranz et al  
583 2012, Huth et al 2015) have been previously studied. The Sentinel-2 image acquisition is  
584 expected to last to last until 2029 (with the potential launch of a complementary twin-satellite  
585 system in 2022) and will allow sustaining the intra-annual data analysis over several seasons

586 (work in progress). Hence the evolution of the vegetation year after year at its maximum  
587 development will be inferred. Hopefully, one will be able to learn from these data and their  
588 correlations with environmental parameters to build predictive models. Other detectors will be  
589 complementary for interannual monitoring such as Rapid Eye, in which archive data were  
590 used in Traganos and Reinartz (2018) in the study of *Posidonia* grass beds.

591

## 592 **Conclusion**

593 In this article, we have presented an off-the-shelf method combining ecological  
594 knowledge and open access remote-sensing technology to monitor the spatial extent of grass  
595 beds in shallow water lagoons over time, with a spatial resolution of 10m and a temporal  
596 frequency of 5 days. The multispectral data are available through the Copernicus Sentinel-2  
597 program, but other detectors could also be used for local peculiarities. Hyperspectral detectors  
598 have been used for wetlands previously, and the linear spectral unmixing analysis method  
599 proposed here is also used in the hyperspectral context (Khanna et al., 2011, Bioucas-Dias et  
600 al., 2013) when different vegetation species may need to be distinguished. Missions using  
601 hyperspectral detectors will be more frequent in the future thanks to recent research and  
602 development efforts. We can cite missions in progress such as PRISMA (ASI), DESIS  
603 (DLR) , in preparation such as EnMAP (DLR) and finally in longer term preparation such as  
604 BG (NASA) and CHIME (ESA).Field survey analysis remains compulsory and is all the more  
605 useful as field campaign dates correspond to image acquisition dates, and the resolution scales  
606 are comparable. In the long term, the continuous survey of the grass beds at a particular  
607 location will allow understanding correlations between water quality, abiotic parameters,  
608 human activity, topography, and biodiversity. Online applications that allow anyone, from  
609 reserve managers to the general public, to follow the system, can be developed easily as is  
610 being done for the Bagnas lagoon training site ([vegmap.irstea.fr](http://vegmap.irstea.fr)).

611

## 612 **Acknowledgments**

613 We thank the staff of the National Natural Reserve of the Bagnas and ADENA for sharing  
614 their knowledge of the reserve, in particular Nathalie Guénel and Julie Bertrand. We thank  
615 Jean-Baptiste Féret, Kenji Ose, Dino Ienco, Marine Le Louarn for insightful discussions on  
616 the topic. Susan Ustin, Shruti Khanna from UC Davis, and Kathy Boyer from SFU in Tiburon  
617 provided insightful information on grass beds monitoring and remote-sensing techniques. We  
618 thank Benjamin Commandré for his efforts to make the results of this work accessible on a  
619 webmapping site under development. MM was supported by a grant from Agence de l'Eau  
620 ("appel a projet Biodiversité 2016"), which also served to finance field surveys. EP wants to  
621 thank the University of Montpellier and LabeX NUMEV through contract AAP2017-1-08.  
622 This research benefited from the support and services of UC Berkeley's Geospatial Innovation  
623 Facility (GIF, [gif.berkeley.edu](http://gif.berkeley.edu)).

624

## 625 **Author contributions**

626 Menu Marion: data curation, analysis, and writing. Papuga Guillaume: fieldwork, data  
627 analysis and writing. Andrieu Frédéric: field work. Debarros Guilhem : visualization. Fortuny  
628 Xavier: writing. Alleaume Samuel: project administration and writing. Pitard Estelle :  
629 conceptualization, supervision, funding acquisition, data analysis, writing. All authors have  
630 reviewed & edited the draft.

631 **References**

632

633 Agbanrin, Y., 2018. Gestion hydraulique de la réserve naturelle du Bagnas (Stage ingénieur).  
634 Ecole Polytechnique, Montpellier.

635 Ahmed, M.H., El Leithy, B.M., Thompson, J.R., Flower, R.J., Ramdani, M., Ayache, F.,  
636 Hassan, S.M., 2009. Application of remote sensing to site characterisation and  
637 environmental change analysis of North African coastal lagoons. *Hydrobiologia* 622,  
638 147–171. <https://doi.org/10.1007/s10750-008-9682-8>

639 Antunes, C., Correia, O., Marques da Silva, J., Cruces, A., Freitas, M. da C., Branquinho, C.,  
640 2012. Factors involved in spatiotemporal dynamics of submerged macrophytes in a  
641 Portuguese coastal lagoon under Mediterranean climate. *Estuarine, Coastal and Shelf*  
642 *Science* 110, 93–100. <https://doi.org/10.1016/j.ecss.2012.03.034>

643 Arzel, C., Elmberg, J., Guillemain, M., 2006. Ecology of spring-migrating Anatidae: a review.  
644 *Journal of Ornithology* 147, 167–184.

645 Benedetti-Cecchi, L., Rindi, F., Bertocci, I., Bulleri, F., Cinelli, F., 2001. Spatial variation in  
646 development of epibenthic assemblages in a coastal lagoon. *Estuarine, Coastal and*  
647 *Shelf Science* 52, 659–668.

648 Bioucas-Dias, Jose & Plaza, Antonio & Camps-Valls, Gustau & Scheunders, Paul &  
649 Nasrabadi, N.M. & Chanussot, Jocelyn. (2013). Hyperspectral Remote Sensing Data  
650 Analysis and Future Challenges. *Geoscience and Remote Sensing Magazine, IEEE*. 1.  
651 6-36. [10.1109/MGRS.2013.2244672](https://doi.org/10.1109/MGRS.2013.2244672).

652 Bradley, D., Thayer, S., Stentz, A., Rander, P., 2004. Vegetation detection for mobile robot  
653 navigation. Robotics Institute, Carnegie Mellon University, Pittsburgh, PA, Tech. Rep. CMU-  
654 RI-TR-04-12.

655 Camacho, A., Peinado, R., Santamans, A.C., Picazo, A., 2012. Functional ecological patterns  
656 and the effect of anthropogenic disturbances on a recently restored Mediterranean  
657 coastal lagoon. Needs for a sustainable restoration. *Estuarine, Coastal and Shelf Science*  
658 114, 105–117. <https://doi.org/10.1016/j.ecss.2012.04.034>

659 Cañedo-Argüelles, M., Rieradevall, M., Farrés-Corell, R., Newton, A., 2012. Annual  
660 characterisation of four Mediterranean coastal lagoons subjected to intense human  
661 activity. *Estuarine, Coastal and Shelf Science, Research and Management for the*  
662 *conservation of coastal lagoon ecosystems* 114, 59–69.  
663 <https://doi.org/10.1016/j.ecss.2011.07.017>

664 Casagrande, C., Boudouresque, C.F., 2007. Biomass of *Ruppia cirrhosa* and *Potamogeton*  
665 *pectinatus* in a Mediterranean brackish lagoon, Lake Ichkeul, Tunisia. *Fundamental and*  
666 *Applied Limnology* 168, 243–255. <https://doi.org/10.1127/1863-9135/2007/0168-0243>

667 Cazals, C., Rapinel, S., Frison, P.-L., Bonis, A., Mercier, G., Mallet, C., Corgne, S., Rudant,  
668 J.-P., 2016. Mapping and characterization of hydrological dynamics in a coastal marsh  
669 using high temporal resolution Sentinel-1A images. *Remote Sensing* 8, 570.  
670 <https://doi.org/10.3390/rs8070570>

671 Chave, P., 2001. The EU Water Framework Directive. IWA Publishing.

672 David, H., 2005. Handbook of biodiversity methods: survey, evaluation and monitoring.  
673 Cambridge University Press.

674 Duarte, P., Bernardo, J.M., Costa, A.M., Macedo, F., Calado, G., Cancela da Fonseca, L.,  
675 2002. Analysis of coastal lagoon metabolism as a basis for management. *Aquatic*  
676 *Ecology* 36, 3–19. <https://doi.org/10.1023/A:1013394521627>

677 Gaertner-Mazouni, N., De Wit, R., 2012. Exploring new issues for coastal lagoons monitoring  
678 and management. *Estuarine, Coastal and Shelf Science* 114, 1–6.  
679 <https://doi.org/10.1016/j.ecss.2012.07.008>

680 Gardner, R.C., Davidson, N.C., 2011. The Ramsar convention, in: LePage, B.A. (Ed.),  
681 *Wetlands: Integrating Multidisciplinary Concepts*. Springer Netherlands, Dordrecht, pp.  
682 189–203. [https://doi.org/10.1007/978-94-007-0551-7\\_11](https://doi.org/10.1007/978-94-007-0551-7_11)

683 GDAL/OGR contributors (2020). GDAL/OGR Geospatial Data Abstraction software Library.  
684 Open Source Geospatial Foundation. URL <https://gdal.org>

685 Gillaranz, L.J., Bascompte, 2012. J. Spatial network structure and metapopulation persistence.  
686 *Journal of Theoretical Biology*, 297, 11-16.

687 Grillas, P., Hilaire, S., Fontès, H., Bec, B., 2018. Campagne de surveillance 2017 de l'état  
688 DCE des lagunes méditerranéennes oligo-et mésohalines françaises pour la physico-  
689 chimie, le phytoplancton et les macrophytes. Consolidation de l'indicateur macrophytes.  
690 Bilan des résultats 2017 (Research Report). Institut de recherche de la Tour du Valat ;  
691 Agence de l'eau Rhône-Méditerranée-Corse 79p.

692 Hagolle, O., Huc, M., Desjardins, C., Auer, S., Richter, R., 2017. MAJA algorithm theoretical  
693 basis document. <https://doi.org/10.5281/zenodo.1209633>

694 Harrell Jr, F.E., 2018. Hmisc: Harrell miscellaneous (Version 4.1-1). Vanderbilt University.

695 Hartog, C., 1981. Aquatic plant communities of poikilosaline waters. *Hydrobiologia* 81, 15–  
696 22.

697 Hiebeler, D., 2004. Competition between far and near disperser in spatially structured  
698 habitats. *Theoretical Population Biology* 66, 205-218.

699 Holm, T.E., Clausen, P., 2006. Effects of water level management on autumn staging  
700 waterbird and macrophyte diversity in three danish coastal lagoons. *Biodiversity and*  
701 *Conservation* 15, 4399–4423. <https://doi.org/10.1007/s10531-005-4384-2>

702 Huth, G., Haegeman, B., Pitard, E., Munoz, F., 2015. Long-distance rescue and slow  
703 extinction dynamics govern multiscale metapopulations. *The American Naturalist* 186,  
704 460.

705 Keshava, N., Mustard, J.F., 2002. Spectral unmixing. *IEEE signal processing magazine* 19,  
706 44–57.

707 Khanna, S., Santos, M.J., Ustin, S.L., Haverkamp, P.J., 2011. An integrated approach to a  
708 biophysically based classification of floating aquatic macrophytes. *International*  
709 *Journal of Remote Sensing* 32, 1067–1094.

710 Kohlus, J., Stelzer, K., Müller, G., Smollich, S., 2020, Mapping seagrass (*Zostera*) by remote  
711 sensing in the Schleswig-Holstein Wadden Sea. *Estuarine, Coastal and Shelf Science*  
712 238, 106699.

713 Lehmann, A., Lachavanne, J.-B., 1997. Geographic information systems and remote sensing  
714 in aquatic botany. *Aquatic Botany* 3, 195–207.

715 Lloret, J., Marín, A., 2009. The role of benthic macrophytes and their associated  
716 macroinvertebrate community in coastal lagoon resistance to eutrophication. *Marine*  
717 *Pollution Bulletin* 58, 1827–1834.

718 Lyons, M.B., Roelfsema, C.M., Phinn, S.R., 2013. Towards understanding temporal and  
719 spatial dynamics of seagrass landscapes using time-series remote sensing. *Estuarine,*  
720 *Coastal and Shelf Science* 120, 42–53.

721 Menéndez López, M., Comín, F.A. (Francisco A.), 1989. Seasonal patterns of biomass  
722 variation of *Ruppia cirrhosa* (Petagna) Grande and *Potamogeton pectinatus* L. in a  
723 coastal lagoon. *Scientia Marina* 53, 633-638.

724 Newton, A., Brito, A.C., Icely, J.D., Derolez, V., Clara, I., Angus, S., Schernewski, G.,  
725 Inácio, M., Lillebø, A.I., Sousa, A.I., Béjaoui, B., Solidoro, C., Tosic, M., Cañedo-  
726 Argüelles, M., Yamamuro, M., Reizopoulou, S., Tseng, H.-C., Canu, D., Roselli, L.,  
727 Maanan, M., Cristina, S., Ruiz-Fernández, A.C., Lima, R.F. de, Kjerfve, B., Rubio-  
728 Cisneros, N., Pérez-Ruzafa, A., Marcos, C., Pastres, R., Pranovi, F., Snoussi, M.,  
729 Turpie, J., Tuchkovenko, Y., Dyack, B., Brookes, J., Povilanskas, R., Khokhlov, V.,  
730 2018. Assessing, quantifying and valuing the ecosystem services of coastal lagoons.  
731 *Journal for Nature Conservation* 44, 50–65. <https://doi.org/10.1016/j.jnc.2018.02.009>

732 Obrador, B., Pretus, J.L., 2010. Spatiotemporal dynamics of submerged macrophytes in a  
733 Mediterranean coastal lagoon. *Estuarine, Coastal and Shelf Science* 87, 145–155.  
734 <https://doi.org/10.1016/j.ecss.2010.01.004>

735 Pereira, P., De Pablo, H., Vale, C., Franco, V., Nogueira, M., 2009. Spatial and seasonal  
736 variation of water quality in an impacted coastal lagoon (Óbidos Lagoon, Portugal).  
737 *Environmental monitoring and assessment* 153, 281–292.

738 Pérez-Ruzafa, A., Marcos, C., Pérez-Ruzafa, I.M., Pérez-Marcos, M., 2011. Coastal lagoons:  
739 “transitional ecosystems” between transitional and coastal waters. *Journal for Coastal*  
740 *Conservation* 15, 369–392. <https://doi.org/10.1007/s11852-010-0095-2>

741 Pojana, G., Gomiero, A., Jonkers, N., Marcomini, A., 2007. Natural and synthetic endocrine  
742 disrupting compounds (EDCs) in water, sediment and biota of a coastal lagoon.  
743 *Environment International* 33, 929–936.

744 Qi, J., Chehbouni, A., Huerte, A.R., Kerr, Y.H., Sorooshian, S., 1994. A modified soil  
745 adjusted vegetation index. *Remote Sensing Environment* 48, 119–126.

746 R Core Team (2019). R: A language and environment for statistical computing. R Foundation  
747 for Statistical Computing, Vienna, Austria. URL <https://www.R-project.org/>.

748 Rodrigo, M.A., Martín, M., Rojo, C., Gargallo, S., Segura, M., Oliver, N., 2013. The role of  
749 eutrophication reduction of two small man-made mediterranean lagoons in the context  
750 of a broader remediation system: Effects on water quality and plankton contribution.  
751 *Ecological Engineering* 61, 371–382. <https://doi.org/10.1016/j.ecoleng.2013.09.038>

752 Santos, M.J., Khanna, S., Hestir, E.L., Greenberg, J.A., Ustin, S.L., 2016. Measuring  
753 landscape-scale spread and persistence of an invaded submerged plant community from  
754 airborne remote sensing. *Ecological applications* 26, 1733–1744.

755 Scheffer, M., 1997. *Ecology of shallow lakes*. Springer Science & Business Media.

756 Schuster, C., Förster, M., Kleinschmit, B., 2012. Testing the red edge channel for improving  
757 land-use classifications based on high-resolution multi-spectral satellite data.  
758 *International Journal of Remote Sensing* 33, 5583–5599.  
759 <https://doi.org/10.1080/01431161.2012.666812>

760 Shili, A., Maïz, N.B., Boudouresque, C.F., Trabelsi, E.B., 2007. Abrupt changes in  
761 *Potamogeton* and *Ruppia* beds in a Mediterranean lagoon. *Aquatic Botany* 87, 181–188.  
762 <https://doi.org/10.1016/j.aquabot.2007.03.010>

763 Silva, T.S.F., Costa, M.P.F., Melack, J.M., Novo, E.M.L.M., 2008. Remote sensing of aquatic  
764 vegetation: theory and applications. *Environmental monitoring and assessment* 140,  
765 131–145. <https://doi.org/10.1007/s10661-007-9855-3>



766 Sutherland, W.J., Adams, W.M., Aronson, R.B., Aveling, R., Blackburn, T.M., Broad, S.,  
767 Ceballos, G., Cote, I.M., Cowling, R.M., Da Fonseca, G.A.B., 2009. One hundred  
768 questions of importance to the conservation of global biological diversity. *Conservation*  
769 *Biology* 23, 557–567.

770 Sutherland, W.J., Fleishman, E., Clout, M., Gibbons, D.W., Lickorish, F., Peck, L.S., Pretty,  
771 J., Spalding, M., Ockendon, N., 2019. Ten years on: a review of the first global  
772 conservation horizon scan. *Trends in Ecology & Evolution* 34, 139-153.  
773 <https://doi.org/10.1016/j.tree.2018.12.003>

774 Therville, C., Mathevet, R., Bioret, F., 2012. Des clichés protectionnistes aux discours  
775 intégrateurs: l’institutionnalisation de réserves naturelles de France. *VertigO* 12:24.

776 Traganos, D., Reinartz, P., 2018. Interannual change detection of mediterranean seagrasses  
777 using rapidEye image time series. *Frontiers in Plant Science* 9, 96.  
778 <https://doi.org/10.3389/fpls.2018.00096>

779 Traganos, D., Reinartz, P., 2018. Mapping Mediterranean seagrasses with Sentinel-2 imagery.  
780 *Marine Pollution Bulletin* 134, 197-209.

781 Van der Maarel, E. (1979). Transformation of cover-abundance values in phytosociology and  
782 its effects on community similarity. *Vegetatio*, 39(2), 97-114.

783 Van Wijk, R.J., 1988. Ecological studies on *Potamogeton pectinatus* L. I. General  
784 characteristics, biomass production and life cycles under field conditions. *Aquatic*  
785 *Botany* 31, 211–258. [https://doi.org/10.1016/0304-3770\(88\)90015-0](https://doi.org/10.1016/0304-3770(88)90015-0)

786 Veetil, B.K., Ward, R.D., Do Amaral Camara Lima M., Stankovic, M., Hoai P.N., Quang  
787 N.X., 2020, Opportunities for seagrass research derived from remote sensing: A review  
788 of current methods, *Ecological Indicators*, 117, 106560.

789 Vis, C., Hudon, C., Carignan, R., 2003. An evaluation of approaches used to determine the  
790 distribution and biomass of emergent and submerged aquatic macrophytes over large  
791 spatial scales. *Aquatic Botany* 77, 187–201. [https://doi.org/10.1016/S0304-](https://doi.org/10.1016/S0304-3770(03)00105-0)  
792 [3770\(03\)00105-0](https://doi.org/10.1016/S0304-3770(03)00105-0)

793 Wikantika, K., Uchida, S., Yamamoto, Y., 2002. Mapping vegetable area with spectral  
794 mixture analysis of the Landsat-ETM, in: *IEEE International Geoscience and Remote*  
795 *Sensing Symposium*. IEEE, pp. 1965–1967.

796 Yamamuro, M., 2012. Herbicide-induced macrophyte-to-phytoplankton shifts in Japanese  
797 lagoons during the last 50 years: consequences for ecosystem services and fisheries.  
798 *Hydrobiologia* 699, 5–19. <https://doi.org/10.1007/s10750-012-1150-9>

799 Zoffoli M.L., Gernez P., Rosa P., Le Bris A., Brando V.E., Barillé A-L., Harin, N, Petrs S,  
800 Poser K., Spaias., Peralta., Barillé, 2020, *Remote Sensing of Environment*, 251, 112020.  
801  
802